Proceedings of the 1999 IEEE/RSJ
International Conference on
Intelligent Robots and Systems

DEVELOPMENT OF BEAM ROTATING ACTUATOR BASED ON VOICE COIL MOTOR TYPE FOR MULTI-BEAM OPTICAL DISC SYSTEM

Cheong Hee Lee, Jung Hyun Lee, Soo Hyun Kim, Yoon Keun Kwak

Department of Mechanical Engineering,
Korea Advanced Institute of Science and Technology,
373-1 Kusong-dong, Yusong-ku, Taejon 305-701, Korea

ABSTRACT

A multi-beam optical disc drive is a method to enhance the data transfer rate in an optical disc system by recording and reading on multi-tracks. In this paper, the beam rotating actuator needed for a multi-beam optical disc drive has been developed.

The Voice Coil Motor(VCM) is used as a driving mechanism for high resolution and small size. Rotating guide based on link structure is designed for frictionless rotation of dove prism.

The characteristics of the actuator is tested through a dynamic analyzer. It shows that the actuator has good linearity, rotating range ±0.34°, minimum resolution of rotating angle 0.0066° and 1st natural frequency 113.9Hz. The actuator is used for a multi-beam optical disc system.

I. INTRODUCTION

The devices that record the various information are necessary in an information-oriented society of the day. An optical disc system that records the information in tracks on a disc using laser is one of the most useful things among these devices. It can store much information, has advantage to noise and is semipermanent.

Many researches have been proceeded to improve the data transfer rate of an optical disc system. There are some methods for the high data transfer rate. First method is to rotate a disc at a high speed. Second method is the development of a fast actuator. Third method is to increase a recording density.[1]~[2]

But the methods that improve an actuating block and a control block using one beam have limits in some measure. At this point of time, a recent trend for high speed of an optical disc system is what use a multi-beam source instead of a existing one-beam system.

In order to use many beams in a multi-beam optical disc system, multi-beam must be collected exactly on tracks recorded information. But beam spots have not formed on multi-tracks simultaneously due to the eccentricity of a disc, the difference of radii of tracks and so on. Therefore a beam rotating actuator is required to compensate for these together with a tracking actuator and a focusing actuator.[3]~[5]

In this paper a beam rotating actuator is newly developed using the dove prism and circular plate springs as rotating guide and is estimated performance based on characteristics of a multi-beam system. Several actuators to be proposed previously are cantilever types, so a beam rotating actuator affects a tracking motion of the multi-beam because a translation of the dove prism coincides with a rotation. It induces an additional load of a tracking actuator. In order to remove this problem, a new beam rotating actuator rotates the dove prism in axis of its geometric center. And the driving source is VCM type to make the actuator have high resolution and small size. Finally the actuator that generates a pure rotation of the multi-beam is developed for a multi-beam optical disc system to improve the data transfer rate.

II. MULTI-BEAM PICK-UP AND DOVE PRISM

II.1 Multi-beam Pick-up

The principle of a multi-beam pick-up is as follows. The multi-beam from a laser diode as beam source passes by a beam splitter and is irradiated in track pits to be recorded the information on a disc by objective lens. And then beams to pass a objective lens and a beam splitter again are collected in a photo diode by an astigmatism lens and transduced to electric signal to read the information. The overall system of a multi-beam pick-up is shown in Fig.1.

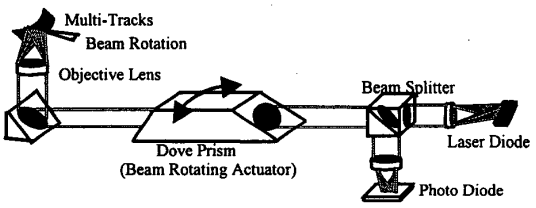

Fig.1 Multi-beam Pick-up

The system needs a beam rotating actuator in a path of the multi-beam to form beam spots on multi-tracks simultaneously. A beam rotating actuator is one of the

most different features of a one-beam system and a multi-beam system.

II.2 Dove Prism

The dove prism is optic parts to rotate image. Therefore the multi-beam can rotate readily by a rotation of the prism. The dove prism is shown in Fig.2 and it is composed of BK7.[6]

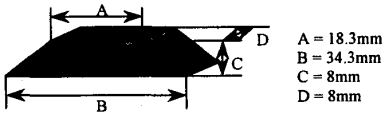

Fig.2 Dove Prism

The size of the dove prism is determined by a effective diameter of passed beams. The size of the prism used in this paper is represented in Fig.2.

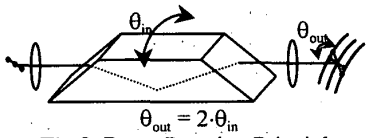

Fig.3 Beam Rotating Principle

The principle of the multi-beam's rotation by the dove prism is shown in Fig.3. The incident beams are refracted downward at the entrance face. The beams are reflected upward from the bottom and then emerge after a second refraction at the exit face. The rotation angle of the multi-beam is twice of that of the prism.

III. DESIGN OF ACTUATOR

III.1 Specifications of Actuator

The tracking breakaway of the multi-beam on a disc is occurred periodically by the eccentricity of a disc and so on. The specifications of the actuator-resolution, rotating range, natural frequency, DC sensitivity- are determined by the errors and the actuator is designed based on the specification.

Resolution. The tracking error has to be below $0.03\mu m$ to regenerate smoothly the information on a disc. Therefore the tracking error of the multi-beam T_e can be expressed as follows

$$T_e = t_e + \Delta t_e \le 0.03\mu m \qquad (1)$$

where t_e is the error by a tracking actuator and Δt_e is that by a beam rotating actuator.

The relation of the rotation of the multi-beam $\Delta\theta$ and the error by a beam rotating actuator Δt_e shown in Fig.4 is as equation(2) because θ_0 and $\Delta\theta$ are small.

$$\Delta t_e = d_b \times [\sin(\theta + \Delta\theta) - \sin\theta] \approx d_b \cdot \Delta\theta \qquad (2)$$

The error by a tracking actuator t_e cannot be below 0.025μm because of limits of the sensor and the controller. Therefore the resolution of a beam rotating actuator must be below 0.015° as follows.

$$\Delta\theta \le \frac{T_e - t_e}{d_b} = 0.015^\circ \qquad (3)$$

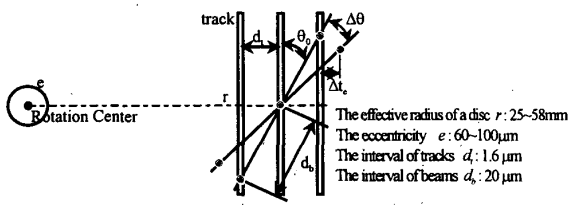

Fig.4 Beam Rotating and Tracking Error

Rotating Range. The reasons to rotate the multi-beam are the eccentricity of a disc, the difference of radii of tracks, the initial rotating angle for optical axis control and so on. The rotating angle of the multi-beam to compensate these is as follows.

$$\theta_b = \theta_1 + \theta_2 + \theta_3 \qquad (4)$$

The rotating angle to compensate for the eccentricity of a disc occurs for the center of a disc and the rotating center are not identical. And the relation of the location change of the multi-beam e_t and the eccentricity e is as follows

$$e_t = e \cdot \sin(\omega t) \qquad (5)$$

where ω is the rotating velocity of a disc. By the radius of disc r and the location change of the multi-beam e_t the rotating angle to compensate for the eccentricity θ_1 is as follows.

$$\theta_1 \approx \frac{e_t}{r} \le \frac{e}{r} \le \frac{100 \times 180}{25000 \times \pi} = 0.23^\circ \qquad (6)$$

Fig.5 shows the arrangement of the multi-beam on tracks. In this configuration, side spots miss tracks by the difference of radii of tracks. The rotating angle of the multi-beam to compensate for that θ_2 is as follows.

$$\theta_2 \le \cos^{-1}\frac{58000^2 + 40^2 - 58003.2^2}{2 \times 40 \times 58000} - \cos^{-1}\frac{25000^2 + 40^2 - 25003.2^2}{2 \times 40 \times 25000} = 0.026^\circ \qquad (7)$$

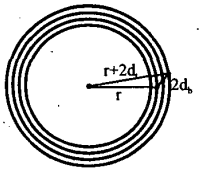

Fig.5 Multi-Beam Array on Disk

And the multi-beam needs to be initially rotated to control the optical axis for initial arrangement. 0.3° is sufficient for the angle θ_3. Namely the overall rotating

angle of the multi-beam θ_b is below 0.56°. Therefore the total rotating range of a beam rotating actuator must be above ±0.28°.

Natural Frequency. The period of the eccentricity of a disc is equal to the rotating period of a disc. So the resonance frequency of the beam rotating block must be above the rotating frequency of a disc.

When the rotating velocity of a disc is considered to 3000rpm, the resonance frequency of the beam rotating block is sufficient if only it is above 50Hz.

DC Sensitivity. The actuator designed in this paper is VCM type. The input is the impressed current i and the output is the rotating angle of the dove prism θ. Because the maximum allowance current in an optical pick-up is about 0.2A, the DC sensitivity of the actuator is as follows.

$$\frac{\theta}{i} \geq \frac{0.28}{0.2} = 1.4\,°/A \qquad (8)$$

III.2 Basic Structure of Actuator

The composition of the actuator is as follows: the dove prism is fixed into the bobbin to wind the coil, the bobbin is supported by the rotating guide at both ends, the magnets are fixed into the case near the coil and all parts are in the case. It is shown in Fig.6.

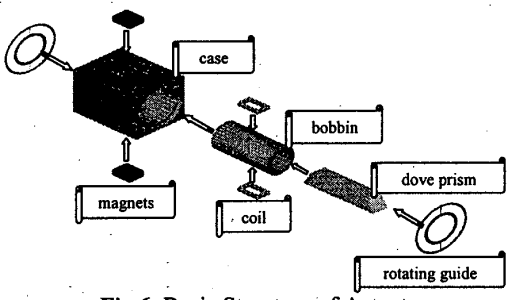

Fig.6 Basic Structure of Actuator

III.3 Magnet and Coil Part

VCM capable of high resolution and small size is applied as the driving source. It is applied to the tracking actuator and focusing actuator, too.

The magnets are arranged near the coil like Fig.7 and the current is applied in same direction at both of the rotating part formed of the dove prism, the bobbin and the coil. Then the forces shown in Fig.7 are generated by Fleming's left-hand rule and rotate the rotating part.

Simulation is executed to get hold of the magnitude of the magnetic force. The size of the magnet is selected so that the effective length of the coil is long. Fig.8 shows the distribution of the magnetic flux density B as the distance x in Fig.7 and Table 1 shows the values of B with changing the distance o at the middle of the magnet, the position of the coil.

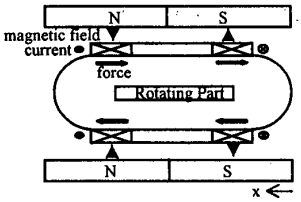

Fig.7 Schematic Diagram of Magnets and coils Part

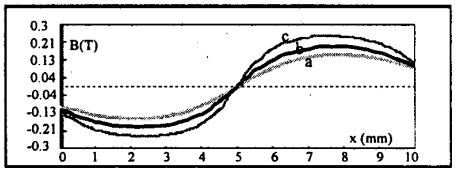

Fig.8 Magnetic Flux Density Distribution

The magnetic flux density B must be as large as possible to decrease the load of the rotating guide. When the interval of the magnet and the coil is below 1.5mm, B of 0.2T is guaranteed.

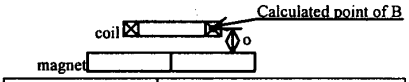

o(mm)	B(T)
2	0.16(c)
1.5	0.2(b)
1	0.24(a)

Table 1. Magnetic Flux Density

III.4 Rotating Guide

The rotating guide is designed so as to lead to a rotation without a translation and be frictionless, axisless and small. So guiding mechanism is based on link structure used widely to design constrained plane motion.

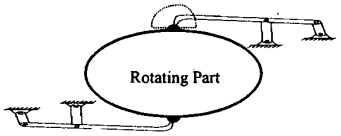

(a) 8 bar Linkage

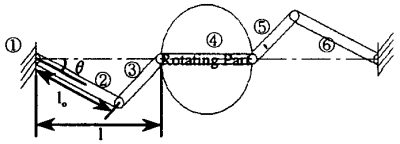

(b) 6 bar Linkage

Fig.9 Link Structures for Rotating Mechanism

Fig.9 shows the link structures for the rotating guide. The 8 bar linkage shown in Fig.9(a) is the structure to

connect the 4 bar linkages to have a linear locus like dashed line with both of the rotating part in order to make a translation motion stiff for a infinitesimal rotation. But this structure is too complex and large for the actuator.
The 6 bar linkage has merits and demerits to be opposite from the 8 bar linkage and is profitable structurally for DC sensitivity. For these reasons the 6 bar linkage is selected and analyzed.

Fig.10 shows the rotation and the translation of the 6 bar linkage. The relation of the input force(F_{in}, $F_{in'}$) and the driving force of link2(F_{out}, $F_{out'}$) is calculated using the method of instant center.

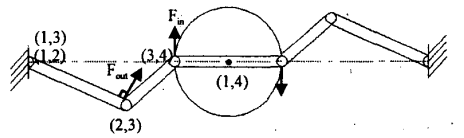

(a) Rotating Motion

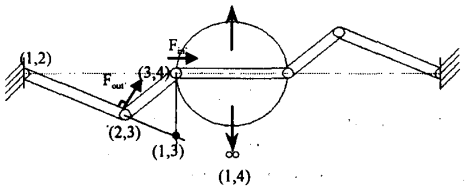

(b) Translating Motion

Fig.10 Comparison between Rotation and Translation

Link4 corresponding to the rotating part rotates in axis of its own center for the rotating motion shown in Fig.10(a). So the instant center of link1 and link4 (1,4) is the center of link4 and the instant center (1,3) is identical to (1,2) as an intersecting point of the line to connect (1,2) with (2,3) and the line to connect (3,4) with (1,4). Therefore the input force for rotating F_{in} and F_{out} are related as follows.

$$\frac{F_{out}}{F_{in}} = \frac{r_{in}}{r_{out}} \cdot \frac{\omega_3}{\omega_2} = \frac{\overline{(1,3)-(3,4)}}{\overline{(1,2)-(2,3)}} \cdot \frac{\overline{(1,2)-(2,3)}}{\overline{(1,3)-(2,3)}} = \frac{l}{l_o} \quad (9)$$

where r_{in} is the distance between the input force and instant center (1,3), r_{out} is the distance between the output force and instant center (1,2).

For the translating motion shown in Fig.10(b), the instant center (1,4) is located in infinity to be perpendicular to the motion and (1,3) is settled similarly to the rotating motion. The input force for translating $F_{in'}$ and $F_{out'}$ are related as follows.

$$\frac{F_{out'}}{F_{in'}} = \frac{\overline{(1,3)-(3,4)}}{\overline{(1,3)-(2,3)}} = \frac{l \cdot \tan\theta}{l/\cos\theta - l_o} = \frac{l \cdot \sin\theta}{l - l_o \cdot \cos\theta} \quad (10)$$

Because the stiffness for the translation must be as large as possible, an angle θ of link2 must be small. Therefore the straight line type of θ=0 is suitable.

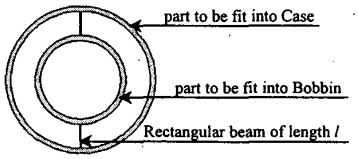

Fig.11 Configuration of Rotating Guide

Fig.11 shows the shape of the rotating guide. It supports to the rotating part at both ends as the circular plate spring type. The length of rectangular beam l is 4.5mm in respect of the overall size of the actuator and the rotating guide is composed of Be-Cu used widely as the material of spring

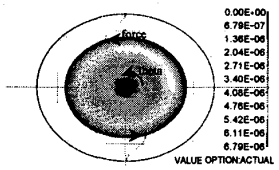

(a) Contour of Beam for Rotation

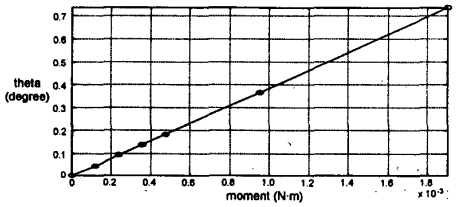

(b) Stiffness for Rotation

Fig.12 FEM Analysis for Rotation

Fig.12 shows the result of simulation for the stiffness of the rotating guide. Fig.12(a) is configuration of the rotating guide when the moment about the center of the rotating part is 0.119E-3 N·m. Forces are applied at points to join the rotating part with the rotating guide when width and thickness of rectangular beam are 0.1mm as the minimum workable dimensions. The relation of the moment and the rotating angle is shown in Fig.11(b). It shows that the relation is linear in the rotating range. The total stiffness of the rotating guide is as follows.

$$K_t = \frac{2 \times 0.119}{1000 \times 0.0458} = 0.0052 \text{ N} \cdot \text{m/deg} \quad (11)$$

III.5 Characteristics Analysis of Actuator

Fig.13 shows the free body diagram of the actuator. The rotating part is rotated by F_c to be generated by the magnets and the coil and M_s is generated by the rotating guide.

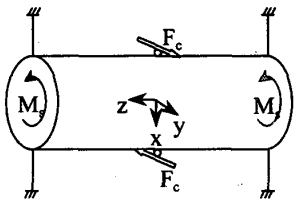

Fig.13 Free Body Diagram of Actuator

The dynamic equation and the natural frequency for rotation are as follows

$$J\ddot{\theta} + C_t\dot{\theta} + K_t\theta = BLd_l i \qquad (12)$$

$$f_\theta = \frac{1}{2\pi}\sqrt{\frac{K_t}{J}} \qquad (13)$$

where J is the mass moment of inertia of the rotating part supposed to a cylinder, C_t is the damping coefficient, d_l is the distance of the coil and the rotating axis and L is the total effective coil length. The length L is 4.8m when the coil is wound by 100 turns around the bobbin at both sides.

Also the static equation and the DC sensitivity are as follows

$$BiLd_l = K_t\theta \qquad (14)$$

$$\frac{\theta}{i} = \frac{BLd_l}{K_t} \qquad (15)$$

When the magnetic flux density and the stiffness simulated previously are substituted into the equations, the characteristics of the actuator are as follows.

f_θ=136.5Hz, θ/i=1.83°/A (16)

It is not good to increase the thickness of the rotating guide because the DC sensitivity is barely 1.3 times of the specification.

IV. CONSTRUCTION OF ACTUATOR

Fig.14 shows the overall appearance of a constructed beam rotating actuator. The magnets are composed of $NdFe_3$ used widely in a small actuator, poly-carbonate is selected as material of the bobbin to make the rotating part light and the diameter of the coil is 0.08mm.

The total size is 30×30×19(mm). The mass of the rotating part and the resistance of the coil connected in series are 8.5g and 37.5Ω.

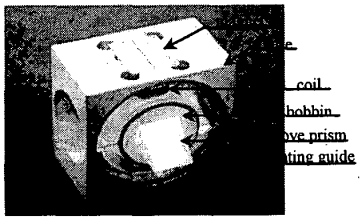

Fig.14 Beam Rotating Actuator

V. EXPERIMENTS

V.1 Static Characteristic of Actuator

Fig.15 shows the experimental setup to measure the rotating angle of the actuator. The beam spot from laser source is reflected by the mirror attached on the dove prism and then is formed on the scale to be distant. The rotating angle of the dove prism is measured by the displacement of the spot on the scale because the angle is small.

The rotating angle θ and the displacement Δx have relation as follows

$$\theta = \frac{1}{2}\cdot\tan^{-1}\left(\frac{\Delta x}{l_m}\right) \approx \frac{\Delta x}{2\cdot l_m} \qquad (17)$$

where the distance of the mirror and the scale l_m is 4.33m.

Fig.16 shows the relation of the inpressed voltage V and the displacement Δx as the result of the rotating angle experiment. The rotating motion of the actuator has linear characteristic. The relation using the least squre method is as follows.

$$\frac{\Delta x}{V} = 6.83\,\text{mm/V} \qquad (18)$$

From the result the DC sensitivity of the actuator is given as equation(19). It has 7.7% error fewly for the analytic value equation(16). For the maximum allowance current 0.2A, the rotating angle of the actuator is ±0.338° to be wider than the specification.

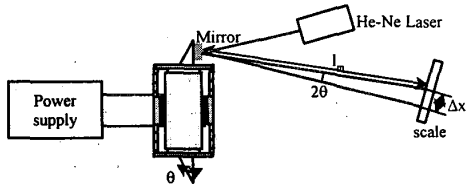

Fig.15 Measurement of Rotating Angle of Dove Prism

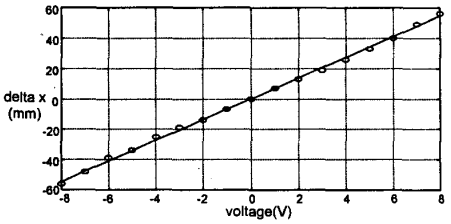

Fig.16 Result of Prism Rotating Experment

$$\frac{\theta}{i} = \frac{\Delta x\cdot R}{2lm\cdot V} = 1.69\ °/\text{A} \qquad (19)$$

The minimun displacement of the spot on the scale is about 1mm for the input voltage V=150mV. Therefore the minimum rotating angle of the actuator is 0.0066° to be 44% level of the specification.

V.2 Dynamic Characteristic of Actuator

Fig.17 shows the experimental setup to measure the dynamic characteristics of the actuator. The swept sine between 5Hz and 1kHz is impressed to the acatuator using the dynamic analyzer *HP35670A*. The power OP amplifier is used as the voltage driver and the laser vibrometer *Polytec OFV1102* senses the rotation of the actuator.

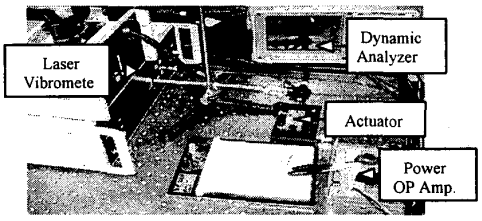

Fig.17 Frequency Response Experiment Set

Fig.18 shows the frequency characteristic of the actuator. The rotating characteristic of the actuator is not affected by other directional motions. The 1st natral frequency is 113.9Hz and the damping ratio is as follows.

$$\zeta = \frac{1}{2 \cdot 10^{(72.1 - 45.7)/20}} = 0.024 \qquad (20)$$

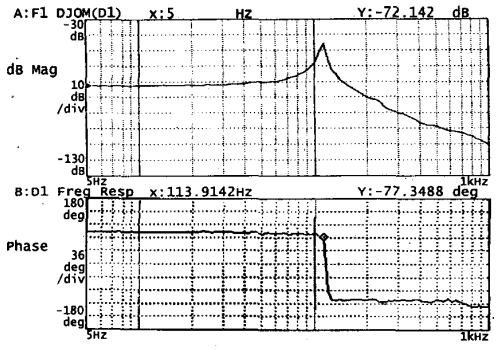

Fig.18 Frequency Response of Actuator

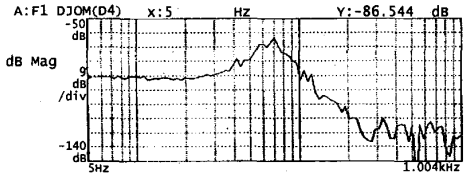

Fig.19 Frequency Response for z-direction

The transfer function of the actuator is given as equation(21) from the natural frequency, the damping ratio and the DC sensitivity.

$$G(s) = \frac{\theta(s)}{I(s)} = \frac{15164}{s^2 + 34.36s + 512288} \qquad (21)$$

Fig.19 shows the frequency characteristic for the translation of the gravitational direction. The plot is defaced somewhat for the displacement is small. Though the natural frequency is below that for the rotation, It does not affect the characteristics of the actuator.

VI. CONCLUSION

A new beam rotating actuator is developed to compensate for a tracking breakaway of beam spots in a multi-beam optical disc system. The dove prism is used to rotate the multi-beam and the driving source is VCM type for high resolution and small size. The specifications of the actuator are based on the tracking errors of the multi-beam by the eccentricity of a disc, the difference of radii of tracks and so on. And the circular plate spring is designed as the rotating guide so as to be frictionless and rotate the dove prism in axis of its geometric center.

The rotating range of the actuator is ±0.338° for the maximum allowance current 0.2A of an optical pick-up and the minimum rotating angle is 0.0066° from the static characteristic experiment.

The 1st natural frequency for the rotation is 113.9Hz without effect of the translation. The transfer function of the actuator is obtained by the dynamic characteristic experiment. Finally it is demonstrated that a developed beam rotating actuator can be applied to a multi-beam optical disc system.

REFERENCES

[1] Koumura, K., Takizawa, F., Iwanaga, T. and Inada, H.(1989), "High Speed Accessing using Split Optical Head," *Optical Data Storage Topical Meeting, Poc. SPIE*, Vol. 1078, pp. 239~243.

[2] Alan B. Marchant(1990), *Optical recording (a technical overview)*, Addison-Welsley Publishing Company, Massachusetts.

[3] Ryuichi Katayama, Kazuhiro Yoshihara and Yutaka Yamanaka(1989), "Multi-beam Mangeto-Optical Disk Drive for Parallel Read/write Operation," *Optical Data Storage Topical Meeting, Proc. SPIE*, Vol. 1078, pp98~104

[4] Haruki Tokumaru, Kiyotaka Arai and Norikazu Kawamura(1996), "Multi-beam optical system Incorporating a Microlens Array," *Jpn, J. Appl. Phys.* Vol. 35, pp375~379.

[5] J.H.Lee(1997), "The Development of the Beam Rotating Actuator Based on the Bimorph Piezo Material," *97' Fall Meeting, Proc. KSPE*, pp. 450~453

[6] Michael Bass, Eric W. Wan Stryland, David R. Williams and William L. Wolfe(1995), *Handbook of Optics*, McGraw Hill Inc. New York